J Sol-Gel Sci Technol (2015) 75:38–44
DOI 10.1007/s10971-015-3672-x

ORIGINAL PAPER

One-step synthesis of carbon-coated $Li_4Ti_{4.95}Nd_{0.05}O_{12}$ by modified citric acid sol–gel method for lithium-ion battery

Chenyang Xia · Changchun Nian · Zhao Huang · Ye Lin · Dan Wang · Chunming Zhang

Received: 16 December 2014 / Accepted: 21 February 2015 / Published online: 31 March 2015

Abstract The effect of Nd doping and one-step carbon coating in $Li_4Ti_{4.95}Nd_{0.05}O_{12}$/C composite materials on the structure and electrochemical performance by modified citric acid sol–gel method was investigated. The obtained samples were characterized by X-ray diffraction, thermogravimetry and transmission electron microscopy. The specific capacities of the $Li_4Ti_{4.95}Nd_{0.05}O_{12}$/C composite at discharge rates of 0.5, 1, 2, 5, 10, 20 and 40 C are 176, 158, 147, 128, 110, 89 and 65 mAh g^{-1}, respectively, which is larger than those of $Li_4Ti_5O_{12}$ and $Li_4Ti_{4.95}Nd_{0.05}O_{12}$ materials at high rates. $Li_4Ti_{4.95}Nd_{0.05}O_{12}$/C also shows excellent cycling performance at high rates after 1000 cycles, which is attributed to its smaller polarization resistance and larger lithium-ion diffusion coefficient than $Li_4Ti_{4.95}Nd_{0.05}O_{12}$ material. The further electrochemical performance was also investigated using electro chemical impedance spectroscopy and cyclic voltammetry.

C. Xia (✉) · C. Nian
School of Information and Electrical Engineering, China University of Mining and Technology, No. 1 Daxue Road, Xuzhou 221008, People's Republic of China
e-mail: bluesky198210@163.com

Z. Huang · C. Zhang
School of Material Science and Engineering, Shanghai Jiaotong University, No. 800 Dongchuan Road, Shanghai 200240, People's Republic of China

Y. Lin
College of Engineering and Computing, University of South Carolina, 301 Main Street, Columbia, SC 29201, USA

D. Wang · C. Zhang (✉)
National Engineering Research Center for Nanotechnology, No.28 East Jiangchuan Road, Shanghai 200241, People's Republic of China
e-mail: zhangchm2003@163.com

Graphical Abstract Carbon-coated $Li_4Ti_{4.95}Nd_{0.05}O_{12}$ could be easily synthesized by the modified citric acid sol–gel method in one step. The $Li_4Ti_{4.95}Nd_{0.05}O_{12}$/C composite exhibited good rate capability and high Li-ion diffusion coefficient. The good performance may partially be derived from the symbiotic impurities such as Li_2TiO_3 and $Li_{0.5}Nd_{0.5}TiO_3$, which is facile for Li^+ diffusion and electron transport.

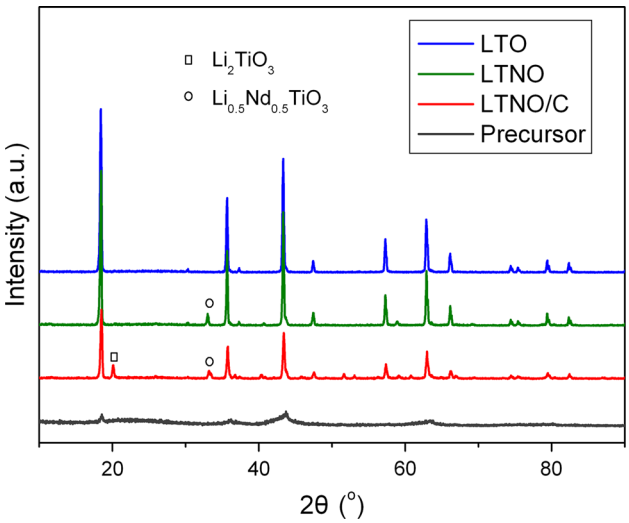

Keywords $Li_4Ti_{4.95}Nd_{0.05}O_{12}$/C · Sol–gel method · Co-chelating agent · Lithium-ion battery

1 Introduction

Rechargeable lithium-ion batteries have been widely used as the power for most portable electronics and considered

as a promising candidate for applications in power storage devices such as electric vehicles (EVs), hybrid electric vehicles (HEVs) and plug-in hybrid electric vehicles (PHEVs) applications [1, 2]. Spinel $Li_4Ti_5O_{12}$ (LTO) material has attracted more attention as anode material for lithium-ion batteries due to its good kinetic performance, unlimited life cycle and high safety with zero strain during charge/discharge processes [3–5]. However, LTO has a weak electric conductivity, which may give a low-rate capacity for high-power batteries.

Recently, in order to solve this problem of LTO, various effective approaches have been proposed: (1) reducing the particle size to nanoscale [6–8]; (2) coating with high electric conductivity such as carbon, metal and metal nitrides powder [9–11]; (3) substituting other metal elements (e.g., Na^+ [12], Mg^{2+} [13], Al^{3+} [14], Cr^{3+} [15], Sc^{3+} [16], Zr^{4+} [17], Nb^{5+} [18], Mo^{6+} [19]) for Li or Ti site. The structure distortion or transition from Ti^{4+} to Ti^{3+} caused by substitution in LTO will lead to an increased electric conductivity and thus improve the high-rate electrochemical performance. Most research in LTO usually focuses on one or two of the above methods, but seldom considering the possible synergy effect. Up to now, the development of more feasible methods to efficiently improve both the nanostructure and electric conductivity by metal ions doping and carbon coating in LTO material remains a big challenge.

In our previous work [16, 20], we reported a modified and facile sol–gel method to prepare 3D LTO with ethylene diamine tetraacetic acid (EDTA) and citric acid (CA) as a bicomponent chelating agent, and further compared the morphology, crystal structure and electrochemical properties of LTO and Sc-doped $Li_4Ti_{4.95}Sc_{0.05}O_{12-\delta}$ (LTSO) anode materials for lithium-ion batteries. However, there are a number of issues still need further exploration, and study on the development of carbon or graphene coating on the surface of electrode material simultaneously remains a challenge. In this work, nano-sized Nd-doped $Li_4Ti_{4.95}Nd_{0.05}O_{12-\delta}$ (LTNO) was also prepared by the modified sol–gel method using EDTA–CA as the bicomponent chelating agent. The influence of Nd^{3+} doping in B site on the lattice structure, and combined with carbon coating on particle size and the electrochemical properties of LTNO are both investigated.

2 Experimental

2.1 Powder synthesis

$Li_4Ti_{4.95}Nd_{0.05}O_{12}$ anode material was synthesized by a modified sol–gel method using EDTA–CA as co-chelating agents [20–22]. A stoichiometric amount of Li_2CO_3, tetrabutyl titanate (TBT) and $Nd(NO_3)_5{\cdot}6H_2O$ were used as raw materials and dissolved into ethanol–HNO_3 pre-blended solution. The mole ratio of Li–Ti–Nd is 4.2:4.95:0.05 and ethanol–HNO_3 is 50:1. In the meantime, the EDTA and CA were pre-dissolved in ammonia, while the mole ratio of total metal ions to EDTA and to CA is 1:1:2. And the ammonia was aimed at keeping solution pH value at about seven. Then, the above solutions were mixed, stirred and heated to 80 °C till the redundant ethanol was evaporated. The resulting transparent gel was heat-treated in an electric oven at 240 °C over 6 h to yield LTNO precursor. The solidified precursor was calcined under open air at 750 °C for 5 h to obtain LTNO powders. The method was also applied to the preparation of LTO. Besides that, the precursor was first calcined under open air at 350 °C for 3 h and then up to 980 °C for 10 h in flowing argon by a tube furnace to obtain LTNO/C.

2.2 Physical characterization

The crystal structures of the synthesized powders were determined by a powder X-ray diffraction (XRD) measurement using a Bruker D8 advance diffractometer with Ni-filtered Cu Kα radiation ($\lambda = 1.5418$ Å) in the 2θ range from 10° to 90°. The amount of the LTNO/C was measured by a thermal gravimetric (TG) method using a TG-DSC analyzer (Model NETZSCH STA449C, Germany) from room temperature to 800 °C at a heating rate of 10 °C min^{-1} in air. The powder morphology was observed using JEOL-2100F transmission electron microscopy (TEM).

2.3 Electrode preparation and electrochemical characterization

The electrochemical cells consisted of Li metal as the anode and LTO-, LTNO- or LTNO/C-based composite oxides as the cathode, which was separated by the porous polypropylene separator (Celgard, 2400), and 1 M solution of $LiPF_6$ in ethylene carbonate (EC)–dimethyl carbonate (DMC)–methyl ethyl carbonate (EMC) was used as the electrolyte (EC–DMC–EMC = 1:1:1, w/w). The working electrode was fabricated by mixing 85:10:5 (w/w) ratio of LTO, LTNO or LTNO/C active material, acetylene black electronic conductor and polyvinylidene fluoride (PVDF) binder, respectively, using *N*-methyl-2-pyrrolidone (NMP) as the solvent. The slurry was then coated on the copper foil ($\sim$10 μm) current collector and dried under vacuum at 120 °C for 12 h. Then, the cells were assembled in a glove box filled with high-purity argon.

The charge/discharge characteristics of the cells were performed over the potential range between 1.0 and 3.0 V using an NEWARE BTS 5 V–10 mA computer-controlled

Galvanostat (Shenzhen, China) at different rates of 0.5–40 °C at room temperature. Electrochemical impedance spectroscopy (EIS) was carried out using an electrochemical workstation (CHI660D) in the frequency range from 0.1 Hz to 1 MHz. Cyclic voltammetry (CV) tests were also performed on this apparatus in the potential window of 1.0–3.0 V versus Li^+/Li at the scanning rate of 0.5 mV s^{-1}.

3 Results and discussion

3.1 Powder characterization

The XRD patterns of the synthesized LTO samples with and without Nd^{3+} doping and carbon coating fired at 750 °C for 5 h are shown in Fig. 1. The precursor of LTNO in Fig. 1a shows an amorphous structure at the probe temperature below 240 °C. All the LTO diffraction peaks are well defined and sharp. It suggests that the sample has good crystallinity, and the synthetic route is correct. The $Li_{0.5}Nd_{0.5}TiO_3$ with perovskite structure was observed when Nd element was doped into the lattice of LTO. It indicates that Nb^{3+} has partially entered the lattice of the spinel. In our previous work, the TG data have proved some free EDTA, CA, NH_4NO_3 and the complex compounds to successive combustion around 280 and 500 °C [20]. It is well known that amorphous carbon could be produced by carbon-containing compound cracking at high temperatures [23]. Therefore, one-step carbon coating and Nd doping of LTNO/C composite materials can be obtained. The precursor of LTNO was first calcined at 340 °C for 1 h in air atmosphere and then at 980 °C for 10 h in flowing argon atmosphere. Compared to LTNO, another miscellaneous material of Li_2TiO_3 was generated. It has been reported that Li_2TiO_3 has three-dimensional path for Li^+ diffusion [24, 25] and then increases the ionic conductivity of LTNO/C composite materials. The XRD pattern of Fig. 1b reveals that the (111) peak of the LTNO and LTNO/C shifted to higher angles. The lattice constant of the LTNO is less than that of the LTO.

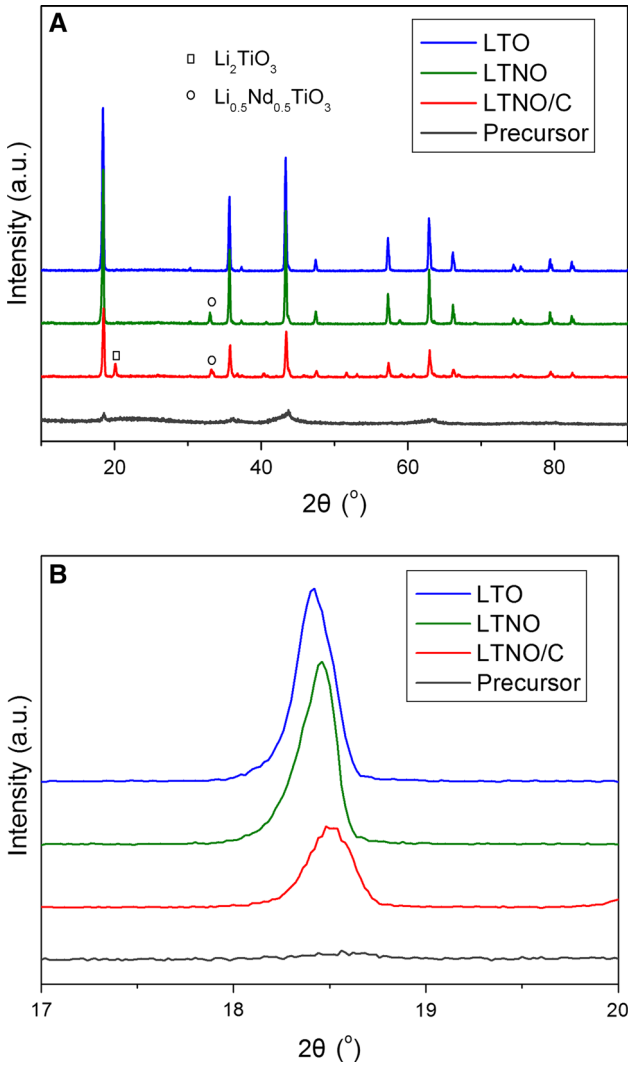

Fig. 1 X-ray diffraction patterns and magnified (111) peaks of precursor, LTO, LTNO and LTNO/C materials prepared by EDTA–CA sol–gel method

Figure 2 shows the TG curve of LTNO/C performed in a flowing air atmosphere between 20 and 800 °C. Three evident steps of weight loss were presented in the TG curve. The first step between room temperature and 210 °C mainly corresponds to the release of water, which is a result of the hygroscopic nature of the sample. The second step is the evaporation of carbon at the temperature range from 210 to 470 °C. The weight loss is 9.84 % in this temperature range. The third step in the temperature range between 470 and 800 °C shows almost no weight loss. This

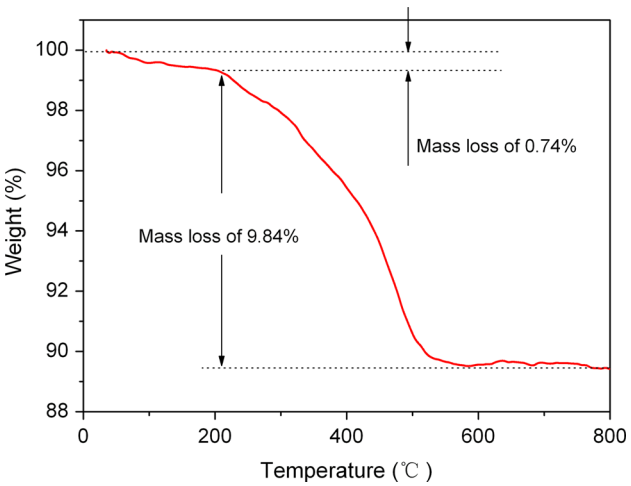

Fig. 2 TG curve of LTNO/C composite material

result indicates that the LTNO crystalline phase stays stable during this temperature range. To further examine the architecture of LTNO/C composite material, the sample was examined by TEM. According to the TEM images shown in Fig. 3a, b, a very thin uniform amorphous carbon layer ($\sim$12 nm) was formed on the LTNO particle surface which is attributed to carbonization of the EDTA and CA organic precursor during calcination in argon atmosphere at high temperature. And the grain size of the as-prepared LTNO/C composite is approximately 250 nm.

3.2 Electrochemical characterization

In order to examine the electrochemical performance of the LTNO/C composite, the initial discharge/charge curves of the LTNO and the LTNO/C electrodes at different current rates from 0.5 to 40 C were firstly carried out. As shown in Fig. 4a, the first discharge capacities reached 176, 158, 147, 128, 110, 89 and 65 mAh g^{-1} corresponding to the discharge rates of 0.5, 1, 2, 5, 10, 20 and 40 C, respectively. The capacities are reduced gradually by the increase in discharge/charge rate. As shown in Table 1 and Fig. 4b, the obtained first specific discharge capacity of LTNO/C is higher than

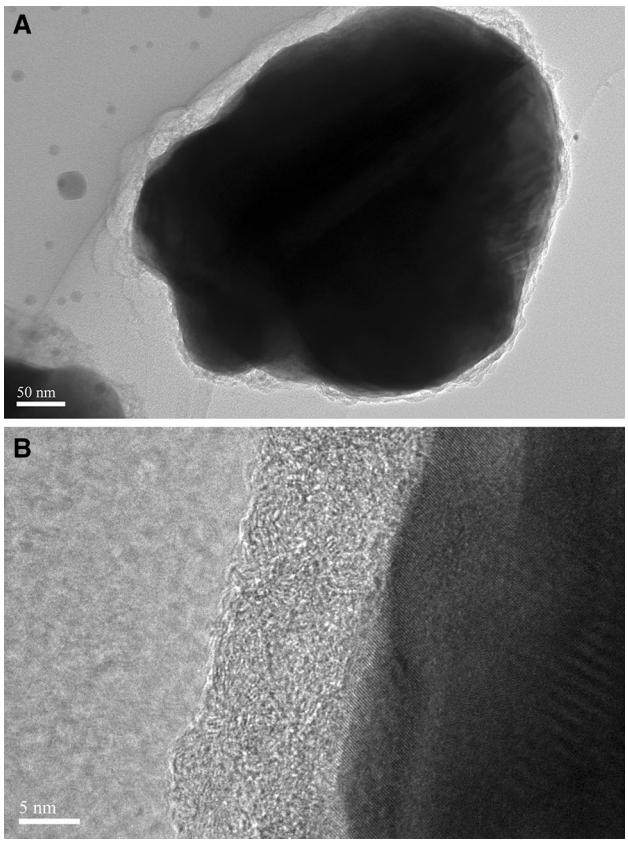

Fig. 3 TEM images of the obtained LTNO/C powder prepared by EDTA–CA sol–gel method

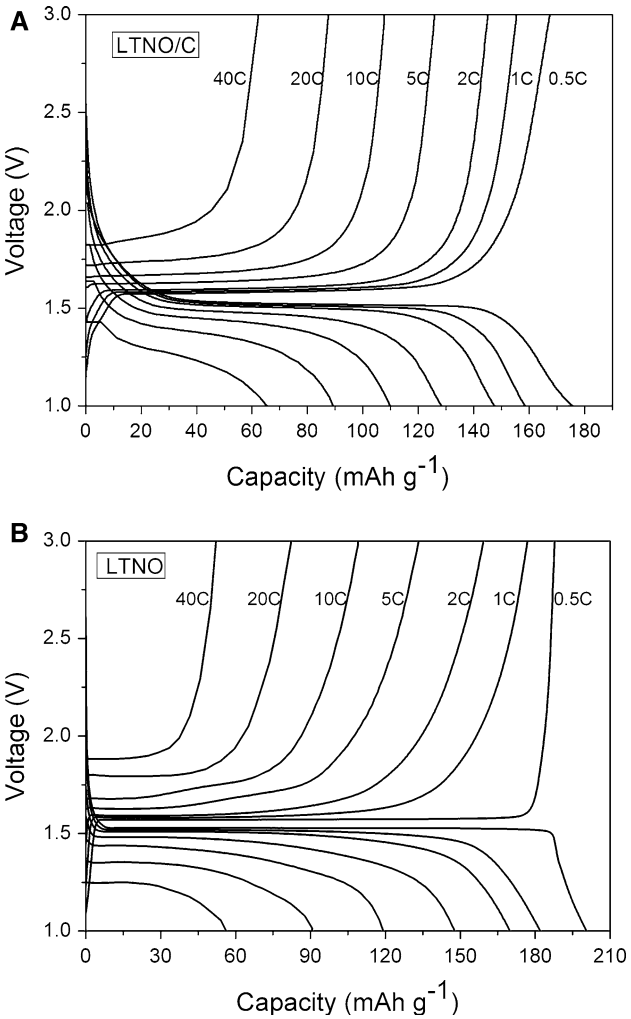

Fig. 4 Variation of the charge/discharge capacities of LTNO (**a**) and LTNO/C (**b**) with the cycle voltage from 1.0 to 3.0 V at different charge/discharge rates between 0.5 and 40 C

LTNO and that reported by our previous work for LTO [20] and La-doped LTO [26]. Figure 5 shows the cycling performance of LTNO and LTNO/C at the rate between 0.5 and 40 C. The LTNO shows much higher discharge capacities during 1–10 C, and the advantage of capacity becomes more narrowly with the increase in the current rates. Meanwhile, it can be seen that carbon-coated LTNO shows the great superiority on specific capacities at high rates (20 and 40 C). The improvement on high-rate capacities of LTNO/C could be related to the improved electric conductivity and the Li^+ insertion/extraction and electronic apparent diffusion rate. Figure 5 also shows that the discharge capacities of LTNO/C are slightly stable with the increasing number of cycling in the range of 1–40 C discharge rates. This could be attributed to the fast reaction kinetics of Li insertion/extraction and electrical transmission.

Then, the cycling behavior of the same cell at the discharge/charge rate at 10 and 20 C within a potential range

Table 1 First discharge capacities of electrode materials prepared by the EDTA–CA sol–gel method and our previous work at the discharge/charge rate range between 0.5 and 40 C

Rate	The first discharge capacity (mAh g^{-1})			
	LTNO	LTNO/C	LTO (reference [20])	$Li_{3.95}La_{0.05}Ti_5O_{12}$ (reference [26])
0.5 C	201	176	181	177
1 C	182	158	164	170
2 C	170	147	156	160
5 C	148	128	139	139
10 C	113	110	108	112
20 C	90	89	76	89
40 C	57	65	49	52

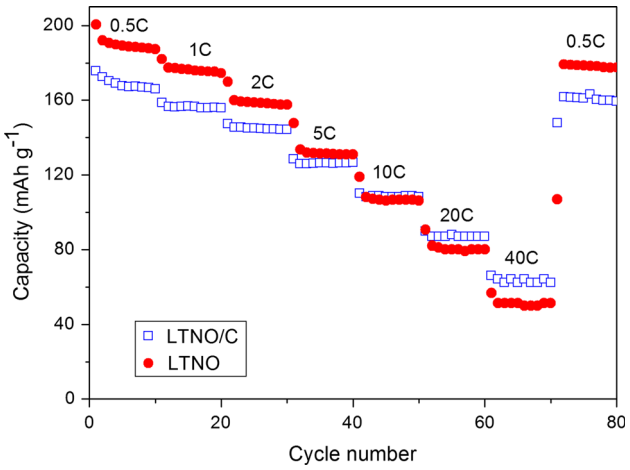

Fig. 5 Ten times cycle performance of LTNO and LTNO/C at the discharge rate range between 0.5 and 40 C within a potential range between 1.0 and 3.0 V

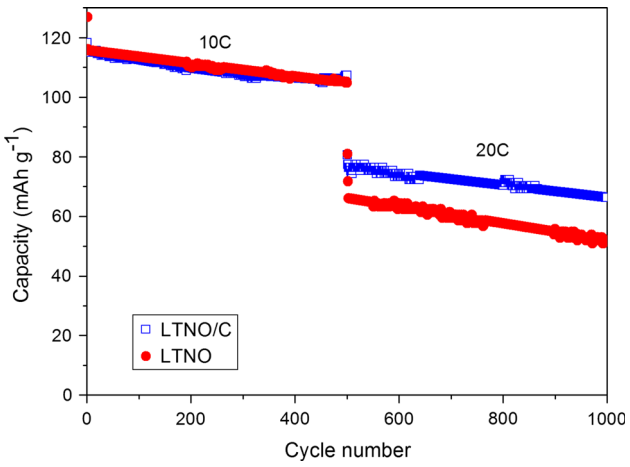

Fig. 6 The 1000 cycles performance of LTNO and LTNO/C at the discharge rate range between 10 and 20 C within a potential range between 1.0 and 3.0 V

between 1.0 and 3.0 V after the above test was further carried out, which was progressively discharged and charged for each 500 cycles in series stages. As shown in

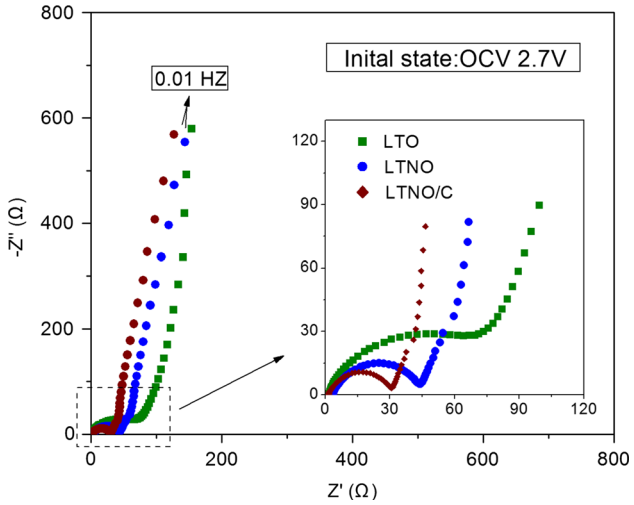

Fig. 7 Electrochemical impedance spectra of the LTO, LTNO and LTNO/C half cells at the original open-circuit voltage of 2.7 V

Fig. 6, the capacities of LTNO and LTNO/C were from 127 and 118 mAh g^{-1} to 105 and 107 mAh g^{-1} at 10 C rate after 500 cycles, respectively. Relatively stable discharged capacities were observed at 10 C rate. The discharge capacity of LTNO/C is significantly higher than that of LTNO after 500 cycles. The capacities of LTNO and LTNO/C were from 81 and 77 mAh g^{-1} to 52 and 66 mAh g^{-1} at 20 C rate after 500 cycles, respectively. The better electrochemical performance of LTNO/C could also be attributed to higher electric conductivity through the modification of carbon thin layer, which led to a faster transmission speed of lithium ions and electrons.

To provide additional information about the differences of LTO, LTNO and LTNO/C, the EIS tests were carried out under open-circuit voltage condition, and the results are presented in Fig. 7. All Nyquist plots showed a depressed semicircle at high frequency and a straight line at low frequency. The depressed semicircle represents the charge transfer resistance at the interface of active material. It can be seen in Fig. 7 that the Nd doping and carbon coating both have a significant impact on the charge transfer

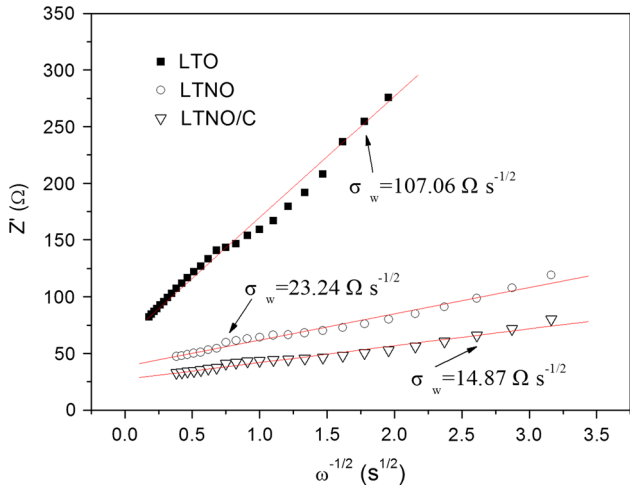

Fig. 8 Relationship between real impedance with the low frequencies of the LTO, LTNO and LTNO/C half cells in the original state

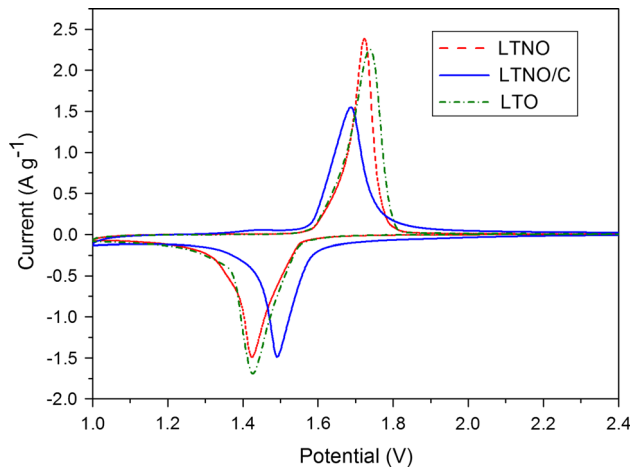

Fig. 9 Cyclic voltammograms of cells using LTO, LTNO and LTNO/C as anode materials at the scanning rate of 0.5 mV s^{-1}

resistance. The charge transfer resistances of LTO, LTNO and LTNO/C are about 86, 42 and 29 Ω. This result indicates that the charge transfer at the electrolyte/electrode interface is greatly improved after Nd doping and the synergy effect of Nd doping and carbon coating. Based on the relationship between the real axis (Z') and the reciprocal square root of the lower angular frequencies ($\omega^{-0.5}$), the Warburg impedance coefficient (σ_w) can be obtained from Fig. 8 and then the Li-ion diffusion coefficient (D) can be calculated according to the Fick's law [27, 28].

$$D = \frac{R^2T^2}{2A^2n^4F^4C^2\sigma_W^2}$$

Here, R is the gas constant, T is the absolute temperature, A is the surface area of the active electrode, n is the number of electrons per molecule during charge/discharge process, F is the Faraday constant, C is the concentration of Li ion. After calculation, the value of D is 2.16×10^{-14}, 4.57×10^{-13} and 1.12×10^{-12} cm^2 s^{-1} for the LTO, LTNO and LTNO/C, respectively.

Figure 9 shows the cyclic voltammograms of cells using LTO, LTNO and LTNO/C as active materials at the scanning rate of 0.5 mV s^{-1} between 1.0 and 3.0 V. The cyclic voltammogram curves of three samples are very similar. Only a pair of reduction and oxidation peaks appears in the cyclic voltammogram curves of LTO, LTNO and LTNO/C. The redox peaks are extremely sharp and well-fined splitting. That means miscellaneous of $LiTi_2O_3$ and $Li_{0.5}Nd_{0.5}TiO_3$ in LTNO and LTNO/C does not affect the oxidation–reduction reactions during charge/discharge process. Furthermore, the cathodic peak corresponding to the voltage platform of the first discharge process in which Li intercalated into the LTNO/C anode is located at ~1.49 V (vs. Li) and the anodic peak corresponding to the voltage platform of the first charge process in which Li deintercalated from the anode is located at ~1.59 V (vs. Li). For pristine LTO and LTNO, the cathodic peak and anodic peak are located at ~1.42/1.74 and ~1.42/1.72 V, respectively. It indicates that Nd doping and carbon coating greatly improve the electrode kinetics characteristics of the LTO electrode. This phenomena confirms that the joint of Nd doping and carbon coating is beneficial to the reversible intercalation and deintercalation of lithium ion.

4 Conclusions

One-step sol–gel approach is designed to synthesize LTNO/C anode material by Nd doping and carbon coating with EDTA–CA as the co-chelating agents. A thin amorphous carbon layer on the LTNO surface and the doped Nd have ameliorating effects on electrochemical properties of active anode material. The specific capacities of LTNO/C are much higher than the corresponding values of LTNO when discharge at high current densities in the voltage range of 1.0–3.0 V. Even at 20 C, the discharge capacity is still retained at 66 mAh g^{-1} after 500 cycles. Furthermore, LTNO/C has been proved to be a high-rate anode material with higher electronic conductivity and lithium-ion diffusivity than LTNO and LTO, implying that Nd doping and carbon coating are beneficial to the reversible intercalation and extraction of Li ion. All the results demonstrate that the LTNO/C electrode is a very promising high-rate anode material for Li-ion batteries.

Acknowledgments This work was supported by "the Fundamental Research Funds for the Central Universities (China University of Mining and Technology) (No. 2014ZDPY17)."

References

1. Goodenough JB, Park KS (2013) J Am Chem Soc 135:1167–1176
2. Armand M, Tarascon JM (2008) Nature 451:652–657
3. Matsui E, Abe Y, Senna M, Guerfi A, Zaghib K (2008) J Am Ceram Soc 91:1522–1527
4. Zhao L, Hu Y, Li H, Wang Z, Chen L (2011) Adv Mater 23:1385–1388
5. Inada R, Shibukawa K, Masada C, Nakanishi Y, Sakurai Y (2014) J Power Sources 253:181–186
6. Kalbác M, Zukalová M, Kavan L (2003) J Solid State Electr 8:2–6
7. Borghols WJH, Wagemaker M, Lafont U, Kelder EM, Mulder FM (2009) J Am Chem Soc 131:17786–17792
8. Zhang N, Liu Z, Yang T, Liao C, Wang Z, Sun K (2011) Electrochem Commun 13:654–656
9. Jung H, Kim J, Scrosati B, Sun Y (2011) J Power Sources 196:7763–7766
10. Sivashanmugam A, Gopukumar S, Thirunakaran R, Nithya C, Prema S (2011) Mater Res Bull 46:492–500
11. Huang S, Wen Z, Zhu X, Yang X (2005) J Electrochem Soc 152:A1301–A1305
12. Yi TF, Yang SY, Li XY, Yao JH, Zhu YR, Zhu RS (2014) J Power Sources 246:505–511
13. Chen CH, Vaughey JT, Jansen AN, Dees DW, Kahalan AJ, Goacher T, Thackeray MM (2001) J Electrochem Soc 148:A102–A104
14. Huang S, Wen Z, Gu Z, Zhu X (2005) Electrochim Acta 50:4057–4062
15. Sun YK, Jung DJ, Lee YS, Nahm KS (2004) J Power Sources 125:242–245
16. Zhang YY, Zhang CM, Lin Y, Xiong DB, Wang D, Wu XY, He DN (2014) J Power Sources 250:50–57
17. Li X, Qu M, Yu Z (2009) J Alloys Compd 487:L12–L17
18. Li H, Shen L, Zhang X, Nie P, Chen L, Xu K (2012) J Electrochem Soc 159:A426–A430
19. Zhang XL, Hu GR, Peng ZD (2011) J Inorg Mater 26:443–448
20. Zhang CM, Zhang YY, Wang J, Wang D, He DN, Xia YY (2013) J Power Sources 236:118–125
21. Zhang CM, Zheng Y, Ran R, Shao ZP, Jin WQ, Xu NP, Ahn J (2008) J Power Sources 179:640–648
22. Shao ZP, Zhang CM, Wang W, Su C, Zhou W, Zhu ZH, Park HJ, Kwak C (2011) Angew Chem Int Ed 50:1792–1797
23. Wang GJ, Gao J, Fu LJ, Zhao NH, Wu YP, Takamura T (2007) J Power Sources 174:1109–1112
24. Lu J, Peng Q, Wang WY, Nan CY, Li LH, Li YD (2013) J Am Chem Soc 135:1649–1652
25. Vijayakumar M, Kerisit S, Yang ZG, Graff GL, Liu J, Sears JA, Burton SD, Rosso KM, Hu JZ (2009) J Phys Chem C 113:20108–20116
26. Wang D, Zhang CM, Zhang YY, Wang J, He DN (2013) Ceram Int 39:5145–5149
27. Ho C, Raistrick ID, Huggins RA (1980) J Electrochem Soc 127:343–350
28. Li B, Han C, He YB, Yang C, Du H, Yang QH, Kang F (2012) Energy Environ Sci 5:9595–9602